Evaluation of the effect of bed thickness in bubbling fluidized beds: CFD-DEM study

Tingwen Li^{1,2*}, Pradeep Gopalakrishnan^{1,3}, Rahul Garg^{1,2}, Mehrdad Shahnam¹

- 1. National Energy Technology Laboratory, Department of Energy, Morgantown, WV 26505, U.S.A.
- 2. URS Corporation, Morgantown, WV 26505, U.S.A.
- 3. Department of Mechanical Engineering, Virginia Tech, Blacksburg, VA 24061, U.S.A.

Abstract

The effect of bed thickness in rectangular fluidized beds is investigated through the CFD-DEM simulations of small-scale systems. Numerical results are compared for bubbling fluidized beds of various bed thicknesses with respect to particle packing, bed expansion, bubble behavior, solids velocities, and particle kinetic energy. Good two-dimensional (2D) flow behavior is observed in the bed having a thickness of up to 20 particle diameters. However, a strong three-dimensional (3D) flow behavior is observed in beds with a thickness of 40 particle diameters, indicating the transition from 2D flow to 3D flow within the range of 20 to 40 particle diameters. Comparison of velocity profiles near the walls and at the center of the bed shows significant impact of the front and back walls on the flow hydrodynamics of pseudo-2D fluidized beds. Hence, for quantitative comparison with experiments in pseudo-2D columns, the effect of walls has to be accounted for in numerical simulations.

Key words: bubbling fluidized bed, CFD, wall effect, discrete element method, pseudo-2D, flow hydrodynamics

^{*} Corresponding author. Tel.: +1 304 285 4538; E-mail address: tingwen.li@ur.netl.doe.gov (Tingwen Li). Mailing address: National Energy Technology Laboratory, Department of Energy, Morgantown, WV 26505, U.S.A.

1. Introduction

Gas-solids fluidized bed reactors are widely used in the chemical industries owing to their excellent gas-solids contact and favorable heat- and mass-transfer characteristics. Continuous efforts have been made during the past decades to gain a thorough understanding of the fundamentals of gas-solids fluidized beds. The literature is abundant with experimental studies on two-dimensional (2D) fluidized beds or pseudo-2D fluidized beds, which are planar rectangular columns of limited thickness. The primary aim of these studies has been to investigate the fundamentals of fluidization, such as bubble properties, flow patterns, and solid mixing, using non-invasive visual or imaging techniques (for example, some recent studies include Caicedo, Marques, Ruiz, & Soler, 2003; Shen, Johnsson, & Leckner, 2004; Pallares & Johnsson, 2006; Busciglio, Vella, Micale, & Rizzuti, 2008; and Hernandez-Jimenez, Sanchez-Delgado, Gomez-Garcia, & Acosta-Iborra, 2011). A great amount of qualitative information gathered from the pseudo-2D beds has been utilized to improve understanding of the flow behavior in three-dimensional (3D) fluidized beds. Moreover, experiments in various pseudo-2D beds provide abundant data for quantitative validation of computational fluid dynamics (CFD) codes.

In a thin pseudo-2D fluidized bed, the front and back walls restrict the solids movement to two dimensions, leading to a quite different flow behavior from a 3D system. For example, the bubble coalescence in a pseudo-2D bed differs from that in a 3D bed, as discussed by Geldart (1970). Additionally, wall frictional effects substantially affect the movements of bubbles and particles. Both effects are attributed to the limited thickness of the pseudo-2D fluidized bed. Various bed thicknesses were reported in the experimental studies of pseudo-2D fluidized beds. For some experiments, the bed thickness was less than 10-particle-diameter to avoid 3D flow behaviors such as variations of velocity components and gradients along the thickness direction (e.g., Hernandez-Jimenez, Sanchez-Delgado, Gomez-Garcia, & Acosta-Iborra, 2011). For such thin bed thicknesses, the frictional effect from the front and back walls could be so significant that particles bridge the bed and give uncharacteristic results (Lyall, 1969). Greater bed thicknesses help to moderate the wall frictional effect. As a general rule, the bed thickness should be less than the characteristic length of the flow, i.e., bubble size, for most studies (Jin & Zhu, 2001). Otherwise, the strong 3D flow pattern due to a great bed thickness causes difficulties in detecting small bubbles using non-invasive visual or imaging techniques. Given the extensive use of pseudo-2D fluidized beds, it is necessary to evaluate the effect of bed thicknesses to better interpret experimental findings.

The effect of bed thickness has mainly been studied with respect to the minimum fluidization velocity, which was consistently shown to increase as the bed thickness decreases (Kathuria & Saxena, 1987; Saxena & Vadivel, 1988; Caicedo, Ruiz, Marques, & Soler, 2002; Sanchez-Delgado, Almendros-Ibanez, Garcia-Hernando, & Santana, 2011). Moreover, it was shown that the minimum fluidization velocity of thin beds depends on the static bed height because of wall friction. Studies by Sanchez-Delgado, Almendros-Ibanez, Garcia-Hernando, & Santana (2011) and Saxena and Vadivel (1988) suggest that the wall effect on the minimum fluidization velocity can be neglected when the ratio between bed thickness and particle diameter exceeds 100. Several discussions on the differences between pseudo-2D and 3D beds can be found in the literature. Geldart (1970) measured the frequency, concentration, and size of bubbles bursting at the surfaces of pseudo-2D and 3D gas-solids fluidized beds. They found that the diameters of bubbles bursting at the surface of a 3D bed were larger than those observed at the surface of a pseudo-2D bed with similar flow conditions. Geldart and Cranfield (1971) measured bubble shapes, sizes, velocities, and concentrations, as well as bed expansion and solid mixing rates in pseudo-2D beds having large particles. In a later study, Cranfield and Geldart (1974) compared the measurements taken

in their 61cm ×2cm bed with the data obtained in a 3D bed with a cross-sectional dimension of 61cm×61cm. They found significant differences between pseudo-2D and 3D beds with respect to voidage at minimum fluidization, \mathcal{E}_{mf} , minimum fluidization velocity, u_{mf} , and minimum bubbling velocity, u_{mh} . Additionally, they reported differences on visible bubble flow, bubble-rising velocity, and bed expansion between pseudo-2D and 3D beds. Rowe and Everett (1972) studied the influence of bed thickness in a rectangular column by varying bed thicknesses from 0.014 m to 0.30 m using X-rays. They estimated the range of bed thicknesses for transition from 2D to 3D behavior and found significant dependence of bubble properties on the bed thickness in the 2D regime. Glicksman and McAndrews (1985) studied the effect of bed thickness with large particles. They reported that the pseudo-2D bed exhibits larger bubbles, higher bubble voidage, and higher visible bubble flow rate than the 3D bed and that the bubbles in a pseudo-2D bed rise more slowly than bubbles of a similar size in the 3D bed. Further, they reported that the bubble behavior was independent of bed thickness if the bed thickness is five times larger than the mean bubble diameter, suggesting the wall effect is negligible. Recently, Lyczkowski, Bouillard, Gamwo, Torpey, & Montrone (2010) investigated the bubble characteristics in a variable-thickness fluidized bed containing horizontal tube bank by comparing absolute and differential pressure fluctuations. Bubble velocities in the thin pseudo-2D bed were found to be 4 to 5 times lower than those in a 3D bed, although bubble diameters were similar in both pseudo-2D and 3D fluidized beds.

In the aforementioned experimental studies, it was clear that direct comparison of detailed flow hydrodynamics between pseudo-2D and 3D beds is very difficult due to limitations in diagnostic tools and measurement techniques. CFD can be a very effective complementary tool to the experiments for achieving a detailed analysis of hydrodynamics in complex gas-solids flows (Grace & Li, 2010). Kawaguchi, Tanaka, and Tsuji (1998) compared discrete element method (DEM) simulations of pseudo-2D fluidized beds using 2D and 3D models to address the wall effect. For a thin fluidized bed (with a ratio between bed thickness and particle diameter of $t/d_n=5$) with a central jet, they reported prominent differences between 2D and 3D models at the beginning of the fluidization process. However, once the fluidization pattern was established, the differences between 2D and 3D model results were limited to the motion of particles near the corner. Busciglio, Vella, Micale, and Rizzuti (2009) conducted 3D simulations of a pseudo-2D bubbling fluidized bed with exact dimensions to assess the suitability of a 2D simulation for predicting the bubble properties in such a system. According to their investigation, there was no significant difference between 2D and 3D simulations as far as the bubble characteristics were concerned. However, no quantitative comparison with respect to the detailed flow hydrodynamics was reported in their study. Feng & Yu (2010) carried out a detailed study to investigate the effect of bed thickness on the segregation behavior of particle mixture in a gas fluidized bed. Both 2D and 3D CFD-DEM simulations were compared in terms of solid flow patterns and microdynamic variables. Their study suggested that both 2D and 3D simulations can capture the key features of the mixing/segregation process, but there exist significant quantitative differences between 2D and 3D simulations. Li, Grace, and Bi (2010) investigated the influence of the solid-phase wall boundary condition by performing 2D and 3D Eulerian-Eulerian numerical simulations of a pseudo-2D bubbling fluidized beds. Their study suggested that the wall effects play an important role in the CFD simulations of pseudo-2D fluidized bed. For this reason, a model that is capable of capturing the particle-wall interaction accurately is needed for numerical simulations. Since particle-wall interaction can be captured more directly by Eulerian-Lagrangian model than Eulerian-Eulerian model, the Eulerian-Lagrangian approach with the flow of particles modeled at particle-scale level, such as DEM, is preferential for studying the effect of bed thickness on the flow hydrodynamics in pseudo-2D fluidized beds.

With the significant improvements in computational power and numerical algorithms, more and more CFD work on multiphase flows can be found in the open literature, and remarkable progress has been made in CFD modeling of gas-solid fluidized beds. In most CFD studies, 2D simulation is used to simulate the flow hydrodynamics in a 3D cylindrical system, which has been shown to work reasonably well for low-velocity fluidization, such as bubbling fluidized bed. On the other hand, 2D simulation is also used to simulate pseudo-2D experiments for predicting the bubble characteristics (Busciglio, Vella, Micale, & Rizzuti, 2009; Li, Grace, & Bi, 2010; Hernandez-Jimenez, Sanchez-Delgado, Gomez-Garcia, & Acosta-Iborra, 2011), and satisfactory agreement between the 2D numerical simulations and the experimental measurements on bubble size distribution and shape factors has been obtained. However, 2D simulations of a pseudo-2D column over-predicted bubble velocity and solid velocity, mainly because of the ignorance of the wall effect from the front and back walls (Li, Grace, & Bi, 2010; Hernandez-Jimenez, Sanchez-Delgado, Gomez-Garcia, & Acosta-Iborra, 2011).

In this study, Eulerian-Langrian simulations of fluidized beds with varying thicknesses are conducted by using an open-source code, MFIX-DEM. The effects of bed thickness on the bubble behavior and solids movement are investigated for a small-scale system. Specifically, the transition from 2D to 3D flow behavior as the bed thickness increases is determined. In addition, a 2D simulation is conducted to reveal the differences between 2D and 3D simulations.

2. MFIX-DEM simulation

2.1. Mathematical models

In MFIX-DEM, the discrete element method (DEM), also known as the discrete particle model (DPM), is used to describe the solids flow at a particle-scale level. The solids phase is represented by actual individual particles in the flow, and inter-particle collisions are directly resolved using the soft-sphere (based on a spring-dashpot model) model of Cundall and Strack (1979) and Tsuji, Kawaguchi, & Tanaka (1993). In the soft-sphere model, collision between particles is treated as a continuous process taking place over a finite time. The contact force is then calculated as a function of the distance between colliding particles based on physically realistic interaction laws using empirical spring stiffness, dissipation constant, and friction coefficient. The particle-wall interaction is treated in the same way as the particle-particle collision. The gas-phase governing equations for mass and momentum conservation are similar to those in the traditional gas-phase-only flow, but with gas volume fraction due to the presence of the solids phase and additional coupling terms due to interactions between the two phases. For the sake of brevity, the full details of governing equations along with the numerical implementation, including the coupling procedure, are not provided here. However, interested readers can find them in Garg, Galvin, Li, & Pannala (2010). A detailed and systematic verification study of MFIX-DEM was conducted and an acceptable level of confidence in the code has been pursued (Garg, Galvin, Li, & Pannala, 2011). Comprehensive validation studies on MFIX-DEM were also conducted through a series of test cases covering a broad range of applications of gas-solids flow (Li, Garg, Galvin, & Pannala, 2011).

2.2. Simulation setup

The fluidized bed geometry chosen for the current study is 10 cm wide and 50 cm high with various thicknesses. Spherical glass beads with diameter and density of 1 mm and 2500 kg/m³ respectively are used in the current

study considering the wide use of glass beads in pseudo-2D fluidized bed experiments. Bed thicknesses of 0.5, 1.0, 2.0, 4.0, and 10 cm, corresponding to 5, 10, 20, 40, and 100 d_p, are simulated. The total particle numbers are 40,000, 80,000, 160,000, 320,000, and 800,000, respectively. The superficial gas velocity is kept constant at 0.8 m/s for all simulations, which is 1.5 times the minimum fluidization velocity, u_{mf} , based on the correlation of Wen & Yu (1966). The 3D computational domain is discretized by a 5-mm uniform grid in each direction. In order to reduce the computational time for the DEM simulation, small spring constants for particle-particle and particle-wall collisions are used, which allows using a large solid time step. The maximum overlap between particles is monitored during the simulation to make sure that no excessive overlap due to small spring constants occurs (van der Hoef, Ye, van Sint Annaland, 2006). The Gidaspow drag law (Gidaspow, 1994) is employed in the whole study to model the interphase momentum transfer. Other parameters used in the simulations are listed in Table 1. A 2D simulation with 8,000 particles is conducted in which the bed thickness of 1-particle-diameter is considered for studying the differences between 2D and 3D modeling. A loosely packed bed formed due to gravity is used as the initial condition for the startup of fluidization. A uniform gas flow is fed through the bottom boundary. The gas flow then leaves the system through the top boundary at a constant pressure. A no-slip boundary condition is used for the gas phase at all side walls. An additional simulation with a free-slip boundary condition for the front and back walls is conducted to evaluate the effect of the gas phase boundary condition.

Table 1.

3. Results and Discussion

To accelerate the computational speed, MFIX-DEM with OpenMP parallelization scheme was utilized. Simulation is conducted on computer node with two Xeon quad-core CPUs running at 2.8 GHz. A total of 10 s of simulation is completed, with transient results recorded at a frequency of 100 Hz for post-processing. To study the effects of bed thickness, results with respect to bed expansion, bubble behavior, and solid velocities of different cases are analyzed after the flow reaches a fully developed state. For further investigation of certain time-averaged quantities, such as mean velocity and mean voidage, the total simulation time is extended for several cases of interest. In addition, results by the 2D DEM simulation are compared with the 3D simulations to address the differences between 2D and 3D modeling.

3.1. Bed expansion

Bed expansion is one of the basic properties of a fluidized bed. The bed expansion ratio is defined as $(H-H_0)/H_0$, where H and H_0 are the bed heights at the expanded and static state, respectively. In the current study, the ratio of the solids loading to the bed cross-sectional area is fixed for all the cases. Before the bed is fluidized, loosely seeded particles are allowed to settle freely under the gravity for 1 second to establish the initial packing state. Figure 1 shows the initial static bed heights for different bed thicknesses. The static bed height decreases sharply with bed thickness up to $t/d_p = 20$, and it becomes independent of bed thickness for $t/d_p > 20$. The higher static bed height for low bed thickness is attributed to the fact that porosity near the wall is higher than porosity in the inner region of a packed bed. The influence of walls on particle packing decreases rapidly as the bed thickness increases. Based on the static bed heights, packing densities can be estimated, which are consistent to the values directly calculated in the simulations. In Figure 1, the datum point obtained from the 2D simulation with a one-

particle-diameter domain is shown for comparison. As no front and back walls are considered in the 2D simulation, the static bed height is lower than that of 3D bed with a thin thickness, i.e., $t/d_p=5$, indicating a higher packing density. However, the static bed height of this one-layer 2D bed is greater than that of 3D beds with $t/d_p > 10$, mainly because of the differences between 2D and 3D sphere-packing structures.

Figure 1.

Through transient snapshots of voidage distribution for different bed thicknesses, bubbling phenomenon is observed in all the cases except for the case with $t/d_p=5$. For $t/d_p=5$, the system behaves like a fixed bed with all particles staying stationary, indicating that no fluidization occurs. Consequently, the minimum fluidization velocity is greater than 0.8 m/s for this bed thickness. It should be noted that the minimum fluidization velocity, u_{mf} determined from the correlation by Wen & Yu (1966) is for 3D beds with negligible wall effect. It has been demonstrated by several studies that the wall friction increases the minimum fluidization velocity as the bed thickness decreases. Sanchez-Delgado, Almendros-Ibanez, Garcia-Hernando, & Santana (2011) developed a correlation for determination of the minimum fluidization velocity in pseudo-2D fluidized beds based on the experimental results obtained in pseudo-2D beds with different particle sizes, bed thicknesses, and bed heights. The ratio between minimum fluidization velocity of a pseudo-2D bed, $u_{mf,2D}$, to that of a 3D bed, u_{mf} , is given as

$$\frac{u_{mf,2D}}{u_{mf}} = \exp\left(a \cdot \left(\frac{d_p}{t}\right)^b\right) \tag{1}$$

where t is the bed thickness, and a and b which are fitting parameters based on the experimental data, reading as 8.5 and 1.6, respectively. Ratios between $u_{mf,2D}$ and u_{mf} for $t/d_p=5$, 10, 20, and 40 are calculated to be 1.91, 1.24, 1.07, and 1.02, respectively. For the case with $t/d_p=5$, the minimum fluidization velocity is predicted to be about 1 m/s, based on this correlation. This is in accordance with the fixed bed behavior predicted by the numerical simulation for $t/d_p=5$. In numerical simulations, it is difficult to measure the expanded bed height due to vigorous eruption of bubbles at the bed surface for most cases. For this reason, the axial profile of the cross-sectional average solids holdup as shown in Figure 2 is generally used to estimate the expanded bed height. However, no systemic conclusion can be obtained from the current results. Additionally, as seen in Figure 2, the solids holdup for the 2D simulation with 1-particle-diameter thickness is similar to that of the 3D simulations. To be more accurate, an average particle height in the fluidized bed proposed by Goldschmidt, Link, Mellema, & Kuipers (2003) is examined. The average particle height is defined as

$$\langle h \rangle = \frac{1}{N} \sum_{i=1}^{N} h_i \tag{2}$$

where h_i is the height of i th particle, and N is the total particle number. The average particle height oscillates due to movement of bubbles. Table 2 depicts the time-averaged values of average particle height over 5 seconds for all cases. The bed expansion behavior is consistent with the solids holdup profile in Figure 3. Only small differences are observed for $t/d_p \ge 10$, which might suggest that the wall effect on bed expansion is negligible once the bed is fluidized. The time-averaged particle height for the case, $t/d_p = 40$, slightly differs from other $t/d_p > 10$ cases. The reason for this deviation is not clear, although it could be that the bed almost completes the

transition from 2D flow to 3D flow at this thickness and starts to present strong 3D bubble behavior. For $t/d_p=5$, the standard deviation of <h> is close to zero as the bed behaves like a fixed bed. It is observed that the eruption of bubbles at the bed surface in the 3D simulations is more vigorous than in the 2D simulation, which explains the slightly lower particle height and standard deviation predicted by the 2D simulation.

Figure 2.

Table 2.

3.2. Bubble behavior

Digital Image Analysis (DIA) is widely used in pseudo-2D fluidized beds to obtain such relevant bubble parameters as bubble size distribution, shape factor, frequency, and rising velocity. However, there are certain limitations in this non-intrusive experimental technique. For example, the bed thickness must be thin enough so that the bubbles span throughout the bed thickness for detection. According to Harrison (1961) and Jackson (1963), a bubble could be as small as a 10-particle-diameter. Hence, the bed thickness should be small enough in order to measure most small bubbles. On the other hand, the ratio of bed thickness to particle diameter should be greater than 10 in order to avoid the particle bridging effects. In this study, we compare the transient bubble behavior of different bed thicknesses to determine the bed thickness suitable for DIA measurement. A threshold value for the voidage is needed to define a bubble. Different values of 0.75, 0.8 and 0.85 have been used in the literature (e.g. Halow, Fasching, Nicoletti, & Spenik, 1993; Kuipers, van Duin, van Beckum, & van Swaaij, 1993; McKeen & Pugsley, 2003). Figure 3 shows the transient iso-surface plot of voidage at 0.75 for different bed thicknesses (similar phenomenon can be observed for voidage of 0.8 and 0.85). For most imaging techniques used in the pseudo-2D fluidized bed experiments, only bubbles open to both walls can be detected. Given this fact, the bubble surface should be normal to the front and back walls for accurate bubble edge detection, which is the case for low bed thicknesses such as $t/d_p=10$ and 20. However, this is not true for greater bed thicknesses, where bubbles demonstrate strong three-dimensional characteristics as shown in Figure 3 (d) for $t/d_p=40$. The bubbles close to the bed surface and attached to the back wall in Figure 3 (d) will not be detected using the imaging technique. Furthermore, even for the bubbles spanning throughout the bed thickness, the bubble diameters might be underestimated during the measurement, as only a portion of the bubble is open to both walls. As far as the 2D bubble behavior is concerned, the bed thickness should not exceed 40-particle-diameter for the small system under consideration. The bubble behavior predicted by the 2D simulation with $t/d_p=1$ is shown in Figure 3 (a) for comparison. Since wall effects are not included in the 2D simulation, the bubble shape differs from that of 3D simulations to certain extent. The bubbles are less spherical and occasionally exceed half of the bed width, behaving like slugs.

Figure 3.

3.3. Solids velocities

Particle Image Velocimetry (PIV) is often used to measure the instantaneous particle velocity in pseudo-2D fluidized beds by coupling with the DIA measurement. Combination of these two non-invasive measuring techniques allows accurate measurement of the mean particle velocity in the dense emulsion phase, as reported

in many experimental studies (e.g., Laverman, Roghair, van Sint Annaland, & Kuipers, 2008; Sanchez-Delgado, Marugan-Cruz, Acosta-Iborra, & Santana, 2010; Hernandez-Jimenez, Sanchez-Delgado, Gomez-Garcia, & Acosta-Iborra, 2011). Since most PIV measurements in fluidized beds are limited to the particles close to the transparent wall, it is critical to understand the difference between the particle velocity along the wall and particle velocity inside the flow field. To this end, the mean particle velocities close to the front wall are compared to those along the middle cut-plane for different bed thicknesses.

In MFIX-DEM simulations, high-frequency data of individual particle position and velocity are generated. In addition, in each computational cell the mean particle velocity used for calculation of the inter-phase coupling due to drag is saved at the same frequency. Due to the coarse computational grid, the mean particle velocity in the Eulerian framework might not be sufficient for investigating the velocity gradient due to the wall effect. Consequently, data of individual particle velocity are analyzed here. The mean particle velocity is simply calculated as

$$\overline{\mathbf{v}}_{s}(x, y, z) = \frac{1}{M} \sum_{i=1}^{M} \mathbf{v}_{i}$$
(3)

M is the number of particles passing a small domain at the position (x,y,z) during a specified time interval. There are different methods to obtain the mean solid velocity. For example, to be consistent with the particle velocity reported in the two-fluid model (TFM) simulations, the mean particle velocity field can be obtained through the time-average of particle velocities in the Eulerian framework. By coupling the voidage distribution and particle-velocity measurement to eliminate the influence of particles raining from the roof of bubbles, one can obtain the same mean particle velocity of the emulsion phase as reported by Laverman, Roghair, van Sint Annaland, & Kuipers (2008). Here, the approach based on Equation (3) is used due to its simplicity. This simple method is enough for revealing the difference between particles velocities close to and far from the wall. Figure 4 presents the profiles of mean vertical particle velocity close to the wall and in the inner region at the height of 40 mm for different bed thicknesses calculated over 5 seconds. For small bed thicknesses of 10dp and 20dp, the difference between particle velocity close to the wall and that along the central cut-plane is quite small, as the friction effect from the front and back walls dominates the flow. The difference becomes significant for greater bed thicknesses as shown in Figures 4(c) and 4(d) since the wall friction dissipates rapidly through a thin shear zone along the wall and becomes less dominant (Nedderman & Laohakul, 1980). Similar results can be obtained for the horizontal component of particle velocity. This result is consistent with the bubble behavior presented before, as bubbling is an important factor driving the solids movement. The transient snapshots of particle velocity in the dense regions are examined and show the same qualitative trend as depicted in Figure 4 for different bed thicknesses.

Figure 4.

3.4. Effect of bed thickness on third dimensional velocity

The effect of walls on the velocity along the thickness of fluidized bed is evaluated by analyzing the kinetic energy of the particles. The mean particle kinetic energy is calculated as the sum of contributions from all three directions.

$$k = k_{x} + k_{y} + k_{z} \tag{4}$$

where k_x , k_y , and k_z are contributions due to the velocity component in the width, height, and thickness directions, respectively, and are calculated as

$$k_{x} = \frac{m}{2N} \sum_{i=1}^{N} u_{i}^{2} \tag{5}$$

$$k_{y} = \frac{m}{2N} \sum_{i=1}^{N} v_{i}^{2} \tag{6}$$

$$k_z = \frac{m}{2N} \sum_{i=1}^{N} w_i^2$$
 (7)

where m is the mass of the particle and N is the total number of particles inside the system. Figure 5 shows the instantaneous variations of k_x , k_y , k_z , and k for $t/d_p=100$ from 5 s to 10 s after the flow is fully developed. As can be seen from the plot, the mean particle kinetic energy fluctuates, presumably due to bubble movements. As seen in Figure 5, the contribution from the vertical particle velocity dominates the mean particle kinetic energy because of the fluidizing gas flow. Due to square cross section of the bed, the contributions from velocities in x and z directions are of similar magnitude.

Figure 5.

The time-averaged mean particle kinetic energy, k, and its z-component, k_z over 5 seconds are reported in Figure 6 (a) for different bed thicknesses. The particle kinetic energy, k, increases with the bed thickness and then levels off at t/d_p =40, while the component, k_z , increases with the bed thickness monotonously. Again, it should be noted that no wall friction from the front and back walls is considered for t/d_p =1, and the result for t/d_p =5 is not included as no particle movement is predicted under such a condition. To further quantify the 3D effect, the ratios k_z/k and k_z/k_x are shown in Figure 6 (b). The z-component contributes less than 2% of the total kinetic energy for t/d_p =10 and 20, and increases to 6% for t/d_p =40 and 15% for t/d_p =100. A similar trend can be observed for k_z/k_x . The results from this study suggest that cases with t/d_p =10 and 20 show good 2D flow behavior, and transition from 2D to 3D occurs around the bed thickness of t/d_p . In this range (20~40dp), it is expected that the wall friction effect starts to dissipate, and the flow is very sensitive to the bed thickness. However, no clear transition can be determined due to the limited bed thicknesses studied here.

Figure 6.

3.5. Further discussions

In the above analyses, the last 5 s of 10 s simulation are used to obtain time-averaged properties, such as bed height, particle velocity profiles, and mean particle kinetic energy. To ensure the results are independent of the

time span used for averaging, simulation time of the case t/d_p =20 has been extended to 30 seconds. Figure 7 shows the time-averaged particle heights and mean particle kinetic energies obtained for different simulation time spans. The average values obtained remain the same for time spans greater than 5 s. However, comparison of time-averaged solid-velocity profiles for different time spans (Figure 8) shows that at least 10 s averaging is required for the mean solid velocity. The velocity profiles shown in Figure 8 are time-averaged based on the solid velocity in each computational cell, which is consistent with the definition used in most literature. It should be noted that the finding depicted in Figure 8 does not affect the conclusion on solid velocities drawn in Section 3.3 since no direct comparison between different cases was used.

Figure 7.

Figure 8.

The boundary condition imposed on the gas phase has been reported to profoundly affect the particle flow behavior in past CFD-DEM simulations of the segregation process of the binary particle mixture in fluidized beds (Beetstra, van des Hoef, & Kuipers, 2007). Hence, different wall boundary conditions for the gas phase at the front and back wall might affect the solids flow, considering the limited grid resolution in the thickness direction. To verify this, the effect of boundary condition for the gas phase has been investigated for the case with t/d_p=20, where no-slip and free-slip boundary conditions at the front and back walls are tested. The effect of those boundary conditions on the left and right walls are not investigated since their effects are of less concern in the current study. Both time-averaged particle height and particle kinetic energy are compared for no-slip and free-slip boundary conditions, and the differences are about 1% only. Figure 9 compares the lateral profiles of the mean vertical particle velocity and voidage at the height of 50 mm, extracted from 20 s simulations. The effect of the gas-phase boundary condition at the front and back walls is negligible for this small bed thickness. It is likely that the effect of the gas-phase boundary condition increases with the bed thickness. Beetstra, van des Hoef, and Kuipers (2007) revealed that the gas phase boundary conditions for the left and right side walls of a pseudo-2D system have a large effect on the segregation behavior, which is not investigated in the current study. Based on their finding, it might be expected that as the bed thickness increases, the effect of gas phase boundary conditions of the front and back walls becomes significant.

Figure 9.

The effect of particle rotation on particle kinetic energy has been evaluated in a similar manner to that of translational kinetic energy. The mean particle rotational kinetic energy is found to be less than 1% of the translational kinetic energy for the case with t/d_p =20. Hence, its effect on the gas-solid flow field has been neglected in the current study. For real systems with non-spherical particles, the particle rotation will be critical and might affect the bubble behavior.

In the current study, the width of the system $(100d_p)$ and ratio of solids loading to the cross sectional area are fixed, and the bed thickness is varied between $5d_p$ and $100d_p$. It is observed that the bed starts to present strong 3D behavior in both bubble and solids flow for t/d_p =40 and the flow in the vicinity of the wall is not representative of the gas-solid flow in the interior of the bed. In order to confirm that the above observations are independent of the width of the bed and solids loading, a simulation with larger bed width $(200d_p)$ and static bed height is performed for t/d_p =40. In this simulation, a total of 1.2 million particles aere simulated. Similar 3D

bubble behavior is observed in the simulation of large bed, especially in the lower region where small bubbles dominate. As far as the 2D bubbles are concerned, the bed thickness should not exceed 40-particle diameters. However, the system with larger width and height does show somehow stronger 2D behavior as the ratio between mean bubble size and bed thickness increases. The mean particle kinetic energy increases by a factor of 2.5 compared to that of the small system because of larger bubbles. At the same time, the ratio of k_z to k is 2%, which is smaller compared to that of the small bed, 6%, suggesting that the increasing width and height promotes the 2D flow behavior to certain extent.

In this study, a 2D simulation (t/dp=1) is presented for comparison with other 3D simulations of various bed thicknesses. Figure 10 compares the time-averaged profiles of vertical solid velocity and voidage at the height of 50 mm, extracted from 20 s simulations for three bed thicknesses. As shown in Figure 10, there exist significant differences between 2D and 3D simulations. In recalling the different bubble behavior presented before, we see that the 2D simulation does not show resemblance to either the thin pseudo-2D bed or the square 3D bed. In addition, there are several limitations of the 2D DEM simulation that should be aware of. It has been generally accepted that there is no good way to determine the voidage in a 2D DEM simulation for the inter-phase drag force calculation (van Wachem, van der Schaaf, Schouten, Krishna, & van den Bleek, 2001). The voidage can be calculated based on the area occupied by the particles in a grid cell. However, this is inconsistent with the empirical correlations for the inter-phase drag force, based on the volume fraction in 3D systems. Hoomans (2000) and Ouyang and Li (1999) proposed similar expressions to convert the 2D voidage based on area to a 3D voidage based on volume, by linking the 2D hexogonal lattice packing to the 3D face-centered cubic (FCC) packing. With this method, the packing density in the dense region tends to be over-predicted by 2D simulations, leading to under-prediction of the minimum fluidization velocity. Alternatively, voidage can be calculated as in a pseudo 3D domain with a thickness of one-particle-diameter, as used by Kawaguchi, Tanaka, & Tsuji (1998) and Xu and Yue (1999). This approach tends to over-predict the minimum fluidization velocity as discussed by Li and Guenther (2011). Li and Guenther (2011) proposed a simple method of linking the 2D particle flow to a 3D system to overcome the under- and over-prediction of particle packing in most 2D DEM simulations. However, their method is quite trivial and needs the experimental measurement on minimum fluidization velocity and voidage for calibration. For these reasons, we simply set the bed thickness to 1-particle diameter for the qualitative investigation in the current 2D simulation. Overall, the 2D DEM simulation is not recommended for quantitative simulation of either pseudo-2D or real 3D systems. However, it can be used as an efficient tool for qualitative study.

Figure 10.

It is necessary to discuss the limitations of this current study and its conclusion. First of all, the numerical simulations conducted are for a small-scale system with relatively coarse particles, and only one flow condition (superficial gas velocity) is considered. Hence, the conclusion drawn from this study might not be applicable to a large system with small particles operating under various flow conditions. No comprehensive parametric study on particle properties, such as density, particle size, and frictional coefficient, was completed due to the high computational cost of DEM simulations. A grid-independent study still needs to be conducted since it has been reported to affect the DEM simulation of segregation. To briefly address the effect of grid resolution in the current study, an additional simulation was conducted for $t/d_p=10$ by using a grid size of $3.3d_p$. The lateral

profiles of mean particle velocity and voidage are shown in Figure 10 for comparison. The results of fine grid differ slightly from that of coarse grid. However, the overall difference is negligible compared to the discrepancy caused by different bed thicknesses. The results of the current study also suffer from the inherent limitations of DEM simulations. For example, perfect spherical particles are used to study the particle-wall interaction, while it is usually expected that the non-spherical particles experience more friction than spheres. Hence, with nonspherical particles, the wall frictional effect might become more evident and propagate farther into the flow. For highly irregular-shaped particles, a thicker bed is recommended to avoid an excessive wall friction effect (Lyall, 1969). In addition, the wall effects on the gas flow are accounted for through particle-gas drag force. However, more detailed effects, limited to 1- or 2-particle layer close the wall, are not captured in DEM simulations. To be more specific, the porosity has a limiting value of unity at the wall, and then its magnitude oscillates with decreasing amplitude away from the wall. DEM is capable of predicting this phenomenon. However, the current CFD model is not able to resolve its influence on the gas flow due to the large grid size required by the CFD-DEM coupling. To fully resolve the gas flow field variation, a first-principle direct numerical simulation (DNS) is needed (e.g. Yu & Shao, 2010; Xiong, Li, Zhou, Fang, Xu, Wang, He, Wang, Wang, Ge, & Li, 2011). However, it is still computationally prohibitive to conduct gas-solids fluidized bed simulations using DNS. Finally, caution should be taken when applying the conclusion from this study to a pseudo-2D system with baffles and tubes, since the insertion of such structure usually promotes the 2D behavior.

4. Conclusions

In this study, we investigated the wall effect on the solids flow behavior in fluidized beds with various thicknesses through numerical simulations. The complex particle-wall interaction is modeled by a particle-scale model, DEM. Based on the numerical results on bubbles, solids velocities, and particle kinetic energy, it is found that cases with bed thickness of $10d_p$ and $20d_p$ present good 2D flow behavior. The bed starts to present significant 3D behavior for the case with a bed thickness of $40d_p$, suggesting the transition from 2D flow to 3D flow occurs between 20~ $40d_p$. The applicability of the conclusion drawn through a small numerical system to a big system has been discussed and limitations of the current study are presented. Due to the inherent limitations of CFD-DEM approach, a direct numerical simulation (DNS) is believed to be preferential to accurately investigate the transition from 2D flow to 3D flow. However, the current study does provide certain insights on the wall effect in pseudo-2D systems with different thicknesses which should be beneficial to design of a 2D experiment and interpretation of the experimental finding. Overall, the friction of front and back walls is demonstrated to have a significant impact on the flow hydrodynamics of pseudo-2D fluidized beds and it cannot be ignored in numerical simulations. For this reason, 2D simulations that ignore the wall effect of pseudo-2D experiments and exclude the effect of a third direction should be used cautiously for quantitative prediction.

Acknowledgments

This technical report was produced in support of the National Energy Technology Laboratory's ongoing research in advanced numerical simulation of multiphase flow under the RES contract DE-FE0004000.

Symbols

d_{p}	Particle diameter	m	
Н	bed height m		
H_0	static bed height	m	
h	particle height	m	
k	kinetic energy	J	
m	particle mass	kg	
N	total particle number	-	
u_{mb}	minimum bubbling velocity m/s		
u_{mf}	minimum fluidization velocity		
v	velocity	m/s	
t	bed thickness	m	
x,y,z	coordinate	m	
Greeks			
δ	standard deviation of particle height		

voidage at minimum fluidization

References:

 \mathcal{E}_{mf}

Beetstra, R., van des Hoef, M.A., & Kuipers, J.A.M. (2007). Numerical study of segregation using a new drag force correlation for polydisperse systems derived from lattice-Boltzmann simulations, *Chemical Engineering Science*, 62, 246-255.

Busciglio, A., Vella, G., Micale, G., & Rizzuti, L. (2008). Analysis of the bubbling behaviour of 2D gas solid fluidized beds Part I. Digital image analysis technique, *Chemical Engineering Journal*, 140, 398–413.

Busciglio, A., Vella, G., Micale, G., & Rizzuti, L. (2009). Analysis of the bubbling behaviour of 2D gas solid fluidized beds Part II. Comparison between experiments and numerical simulations via digital image analysis technique, *Chemical Engineering Journal*, 148, 145–163.

Caicedo, G.R., Ruiz, M.G., Marques, J.J.P., & Soler, J.G. (2002). Minimum fluidization velocities for gas-solid 2D beds, *Chemical Engineering and Processing*, 41, 761-764.

Caicedo, G.R., Marques, J.J.P., Ruiz, M.G., & Soler, J.G. (2003). A study on the behaviour of bubbles of a 2D gas—solid fluidized bed using digital image analysis, *Chemical Engineering and Processing*, 42, 9–14.

Cranfield, R.R., & Geldart, D. (1974). Large particle fluidisation, Chemical Engineering Science, 29, 935-947.

Cundall, P. A., & Strack, O.D.L. (1979). A discrete numerical model for granular assemblies, *Geotechnique*, 29, 47-65.

Feng, Y.Q., & Yu, A.B. (2010). Effect of bed thickness on the segregation of particle mixtures in a gas fluidized bed, *Industrial & Engineering Chemistry Research*, 49, 3459-3468.

Garg, R., Galvin, J., Li, T., & Pannala, S. (2010). Documentation of open-source MFIX-DEM software for gassolids flows. online documentation, https://mfix.netl.doe.gov/documentation/dem_doc_2010.

Garg, R., Galvin, J., Li, T., & Pannala, S. (2011). Open-source MFIX-DEM software for gas-solids flows: Part I – verification studies, *Powder Technology*, doi: 10.1016/j.powtec.2011.09.019.

Geldart, D. (1970). The size and frequency of bubbles in two- and three-dimensional gas-fluidised beds, *Powder Technology*, 4, 41-55.

Geldart, D., & Cranfield, R.R. (1972). The gas fluidization of large particles, *Chemical Engineering Journal*, 3, 211-231.

Gidaspow, D. (1994). *Multiphase flow and fluidization: continuum and kinetic theory descriptions*. Boston: Academic Press.

Glicksman, L.R., & McAndrews, G. (1985). The effect of bed width on the hydrodynamics of large particle fluidized beds, *Powder Technology*, 42, 159-167.

Goldschmidt, M.J.V., Link, J.M., Mellema, S., & Kuipers, J.A.M. (2003). Digital image analysis measurements of bed expansion and segregation dynamics in dense gas-fluidised beds, *Powder Technology*, 138, 135-159.

Grace, J.R., & Li, T. (2010). Complementarity of CFD, experimentation and reactor models for solving challenging fluidization problems, *Particuology*, 8, 498-500.

Halow, J.S., Fasching, G.E., Nicoletti, P., & Spenik, J.L. (1993). Observations of a fluidized-bed using capacitance imaging. *Chemical Engineering Science*, 48, 643–659.

Harrison, D., Davidson, J.F., & Kock, J.W. (1961). On the nature of aggregative and particulate fluidisation, *Chemical Engineering Research and Design*, 39, 202–211.

Hernandez-Jimenez, F., Sanchez-Delgado, S., Gomez-Garcia, A., & Acosta-Iborra, A. (2011). Comparison between two-fluid model simulations and particle image analysis & velocimetry (PIV) results for a two-dimensional gas-solids fluidized bed, *Chemical Engineering Science*, 66, 3753-3772. Hoomans, B.P.B. (2000). *Granular dynamics of gas-solid two-phase flows*, Enschede.

Jackson, R. (1963). The mechanics of fluidised beds, Chemical Engineering Research and Design, 41, 13–21.

Jin, Y., & Zhu, J. (2001). Principle of fluidization engineering, Beijing; Tsinghua University Press.

Kathuria, D.G., & Saxena, S.C. (1987). A variable-thickness two-dimensional bed for investigating gas-solid fluidized bed hydrodynamics, *Powder Technology*, 53, 91-96.

Kawaguchi, T., Tanaka, T., & Tsuji, Y. (1998). Numerical simulation of two-dimensional fluidized beds using the discrete element method (comparison between the two- and three-dimensional models), *Powder Technology*, 96, 129-38.

Kuipers, J.A.M., van Duin, K.J., van Beckum, F.P.H., & van Swaaij, W.P.M. (1993). Computer simulation of the hydrodynamics of a two-dimensional gas-fluidized bed. *Computers & Chemical Engineering*, 17, 839–858.

Laverman, J.A., Roghair, I., van Sint Annaland, M., & Kuipers, H. (2008). Investigation into the hydrodynamics of gas-solid fluidized beds using particle image velocimetry coupled with digital image analysis, *Canadian Journal of Chemical Engineering*, 86, 523-535.

Li, T., & Guenther, C. (2011). MFIX-DEM simulations of change of volumetric flow in fluidized beds due to chemical reactions, *Powder Technology*, doi: 10.1016/j.powtec.2011.09.025.(in press).

Li, T., Grace, J.R., & Bi, X. (2010). Study of wall boundary condition in numerical simulations of bubbling fluidized beds, *Powder Technology*, 203, 447-457.

Li, T., Garg, R., Galvin, J., & Pannala, S. (2011). Open-source MFIX-DEM software for gas-solids flows: Part II – validation studies, *Powder Technology*, doi: 10.1016/j.powtec.2011.09.020.

Lyall, E. (1969). The photography of bubbling fluidised beds, British Chemical Engineering, 14, 501-506.

Lyczkowski, R.W., Bouillard, J.X., Gamwo, I.K., Torpey, M.R., & Montrone, E.D. (2010). Experimental and CFD analyses of bubble parameters in a variable-thickness fluidized bed, *Industrial & Engineering Chemistry Research*, 49, 5166-6173.

McKeen, M., & Pugsley, T. (2003). Simulation and experimental validation of a freely bubbling bed of FCC catalyst. *Powder Technology*, 129, 139–152.

Nedderman, R.M., & Laohakul, C. (1980). The thickness of the shear zone of flowing granular materials, *Powder Technology*, 25, 91-100.

Ouyang, J., & Li, J. (1999). Particle-motion-resolved discrete model for simulating gas-solid fluidization, *Chemical Engineering Science*, 54, 2077-2083.

Pallares, D., & Johnsson, H. (2006). A novel technique for particle tracking in cold 2-dimensional fluidized beds — simulating fuel dispersion, *Chemical Engineering Science*, 61, 2710–2720.

Rowe, P.N., & Everett, D.J. (1972). Fluidised bed bubbles viewed by X-rays Part II- The transition from two to three dimensions of undisturbed bubbles, *Chemical Engineering Research and Design*, 50, 49-54.

Sanchez-Delgado, S., Marugan-Cruz, C., Acosta-Iborra, A., & Santana, D. (2010). Dense-phase velocity fluctuation in a 2-D fluidized bed, *Powder Technology*, 200, 37-45.

Sanchez-Delgado, S., Almendros-Ibanez, J.A., Garcia-Hernando, N., & Santana, D. (2011). On the minimum fluidization velocity in 2D fluidized beds. *Powder Technology*, 207, 145-153.

Saxena, S.C., & Vadivel, R. (1988). Wall effects in gas-fluidized beds at incipient fluidization, *Chemical Engineering Journal*, 39, 133-137.

Shen, L.H., Johnsson, F., & Leckner, B. (2004). Digital image analysis of hydrodynamics two dimensional bubbling fluidized beds, *Chemical Engineering Science*, 59, 2607–2617.

Tsuji, Y., Kawaguchi, T., & Tanaka, T. (1993). Discrete particle simulation of two-dimensional fluidized bed. *Powder Technology*, 77, 79-87.

van Wachem, B.G.M., van der Schaaf, J., Schouten, J.C., Krishna, R., van den Bleek, (2001). Experimental validation of Lagrangian-Eulerian simulations of fluidized beds, *Powder Technology*, 116, 155-165.

van der Hoef, M.A., Ye, M., van Sint Annaland, M., Andrews IV, A.T., Sundaresan, S., & Kuipers, J.A.M. (2006). Multiscale modeling of gas-fluidized beds, *Advances in Chemical Engineering*, 31, 65-149.

Wen, C.Y., & Yu, Y.H. (1966). A generalized method for predicting the minimum fluidization velocity, *AIChE Journal*, 12, 610-612.

Xiong, Q., Li, B., Zhou, G., Fang, X., Xu, J., Wang, J., He, X., Wang, X., Wang, L., Ge, W., & Li, J. (2011). Large-scale DNS of gas-solid flows on Mole-8.5. *Chemical Engineering Science*, doi: 10.1016/j.ces.2011.10.059.

Xu, B.H., & Yu, A.B. (1997). Numerical simulation of the gas-solid flow in a fluidized bed by combining discrete particle method with computational fluid dynamics. *Chemical Engineering Science*, 52, 2785-809.

Yu, Z., & Shao, X. (2010). Direct numerical simulation of particulate flows with a fictitious domain method, *International Journal of Multiphase Flow*, 36, 127-134.

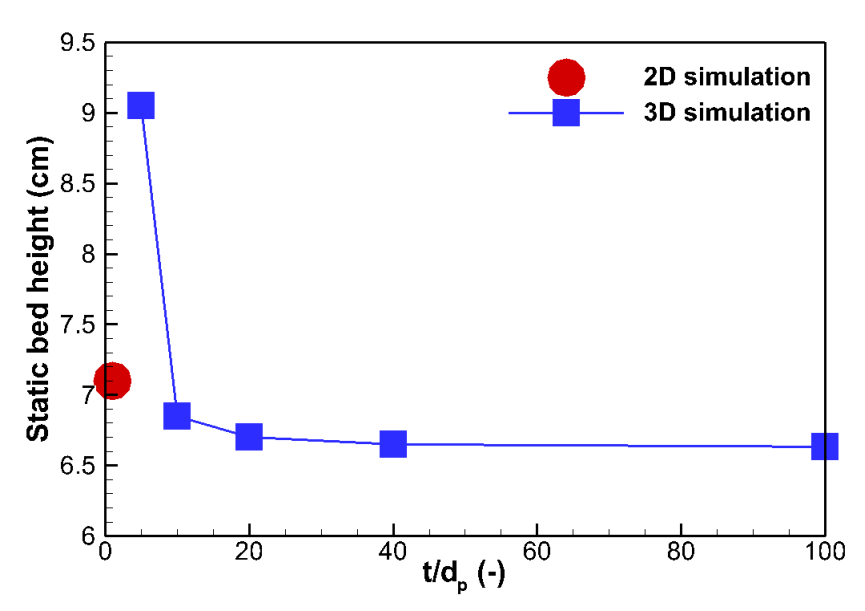


Figure 11. Static bed heights for different bed thicknesses.

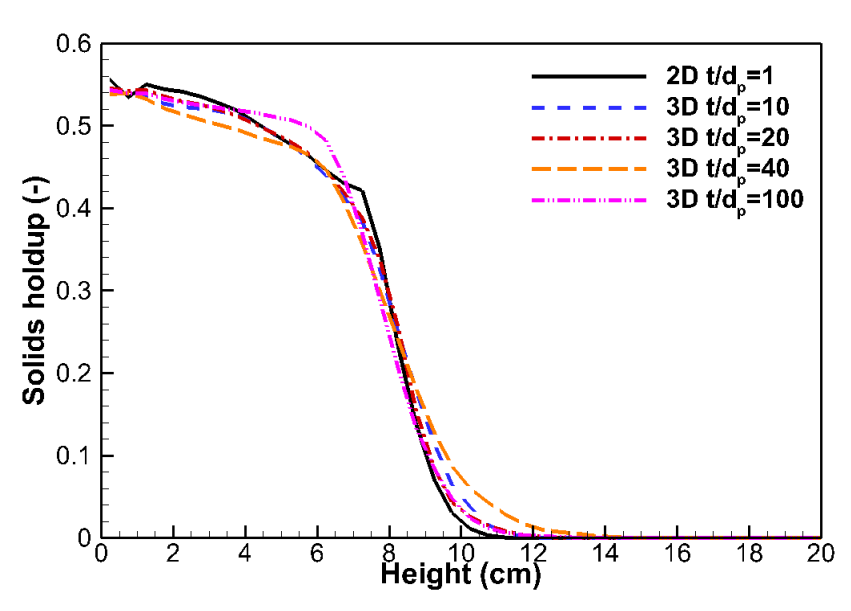


Figure 12. Axial profiles of cross-sectional average solids holdup for different bed thicknesses.

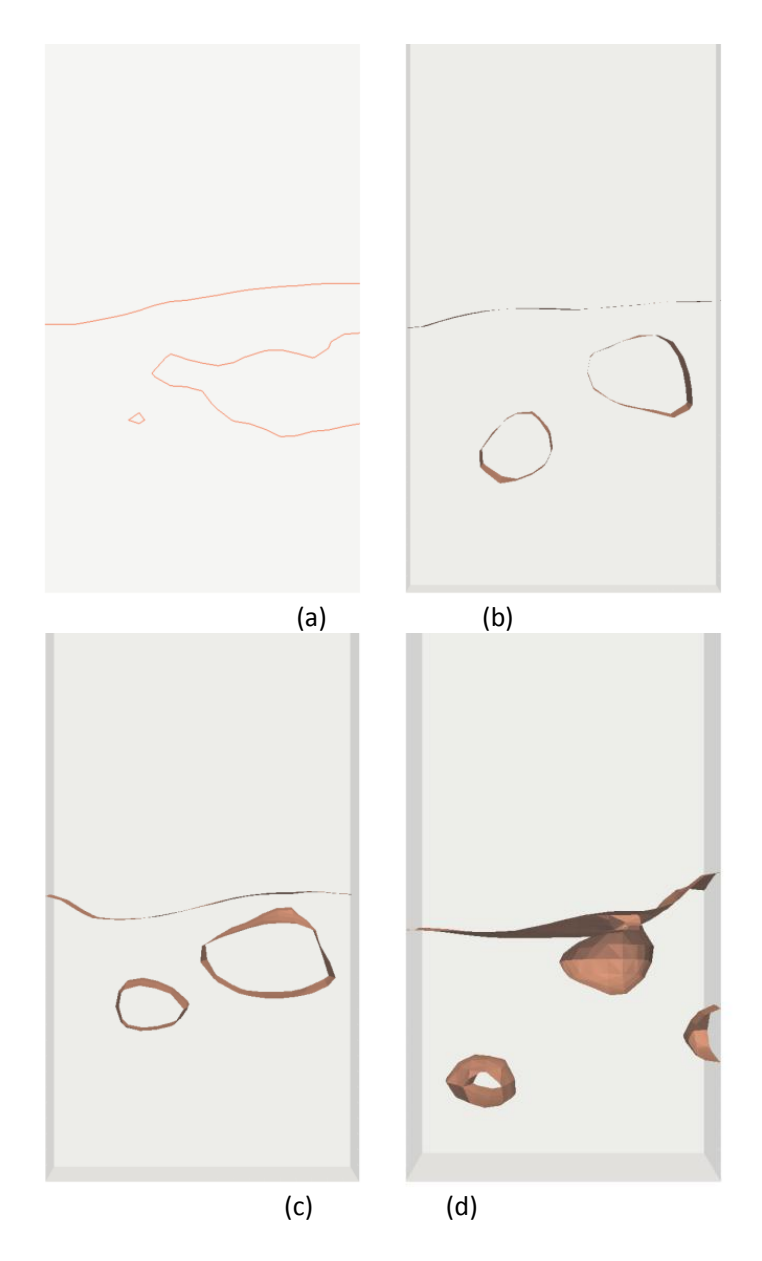
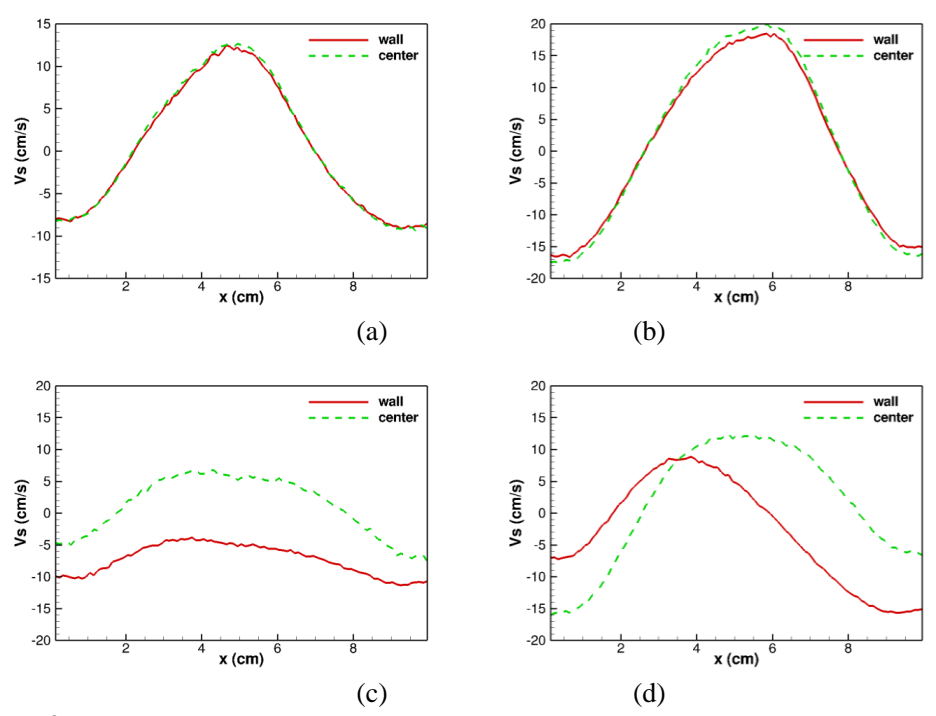


Figure 13. Transient snapshots of bubble behavior for different bed thicknesses (iso-surface of voidage of 0.75): (a) $t/d_p=1$, 2D; (b) $t/d_p=10$; (c) $t/d_p=20$; (d) $t/d_p=40$.



(c) (d) Figure 14. Profiles of mean vertical particle velocities over 5s close to the wall and in the inner region at the height of 40 mm for different bed thicknesses: (a) $t/d_p=10$; (b) $t/d_p=20$; (c) $t/d_p=40$; (d) $t/d_p=100$.

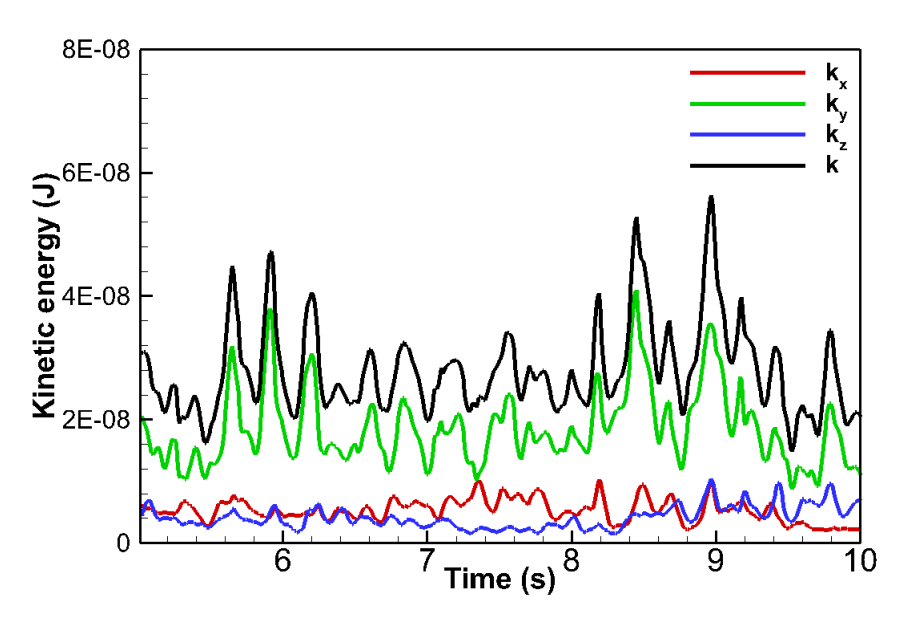


Figure 15. Variations of k_{x} , k_{y} , k_{z} and k for t/d_p=100 after the flow is fully developed.



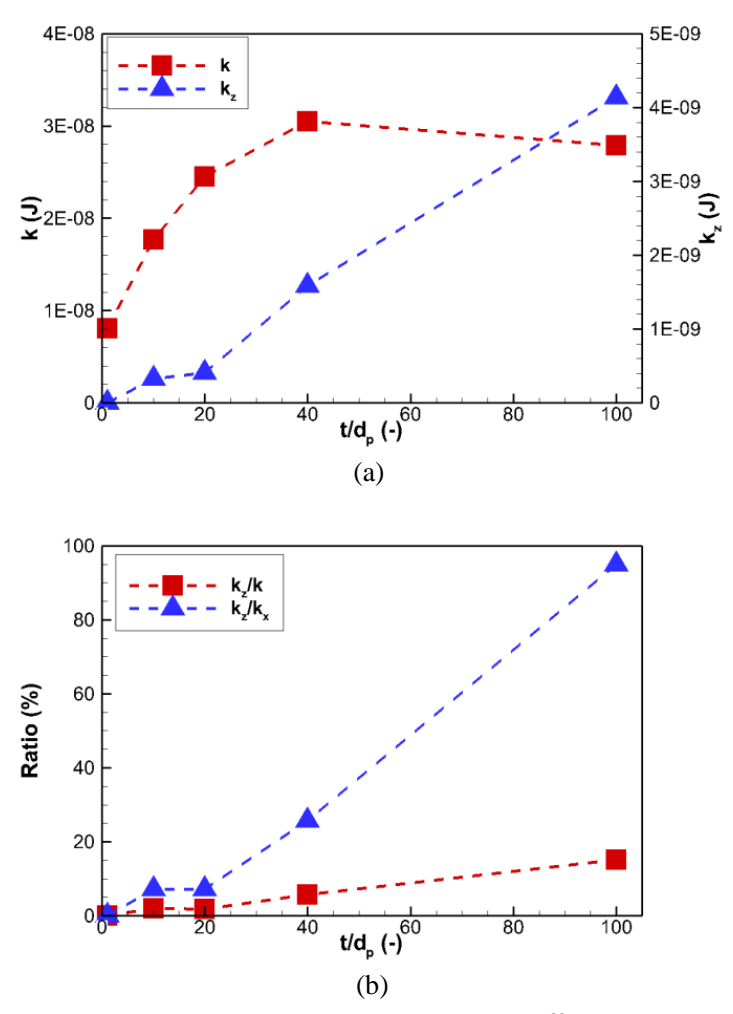


Figure 16. Variation of mean particle kinetic energy and ratios between different components: (a) variation of k and k_z with bed thickness; (b) k_z/k and k_z/k_x for different bed thicknesses.

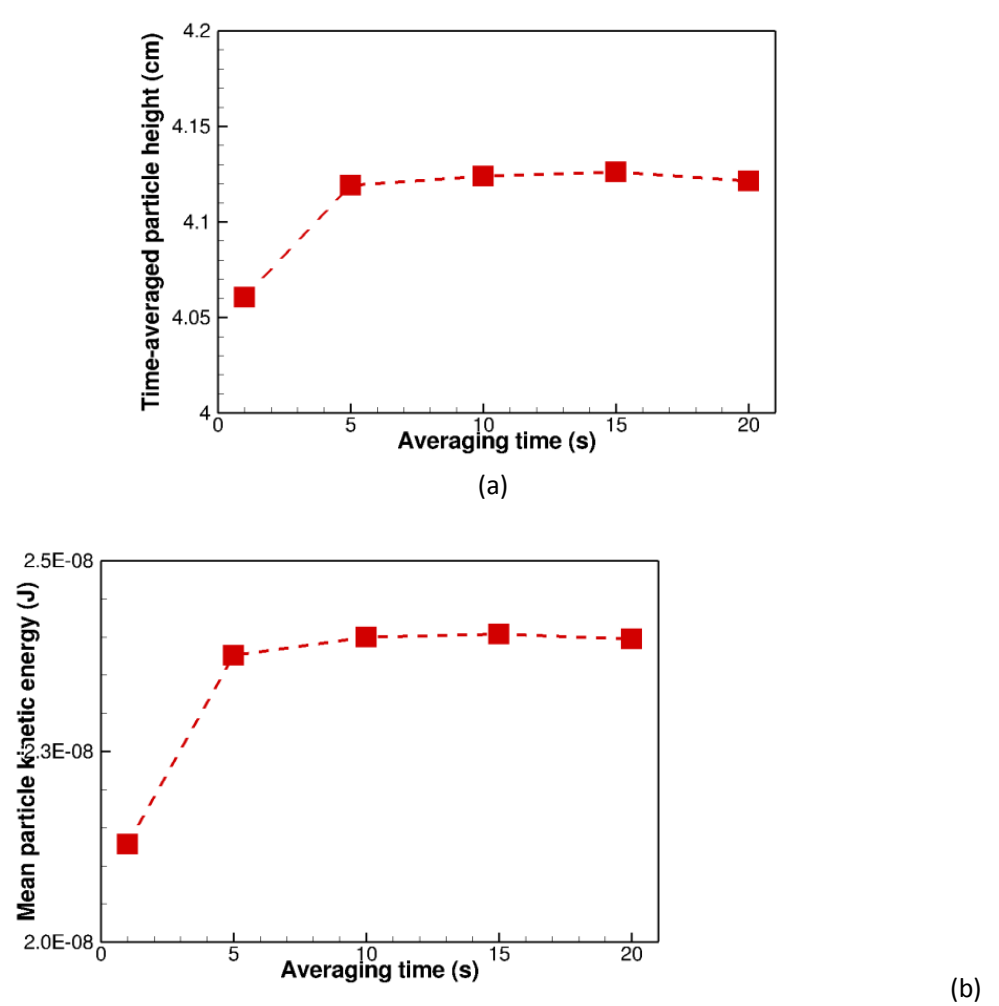


Figure 17. Variations of time-averaged particle height and mean particle kinetic energy for different averaging time spans ($t/d_p=20$).

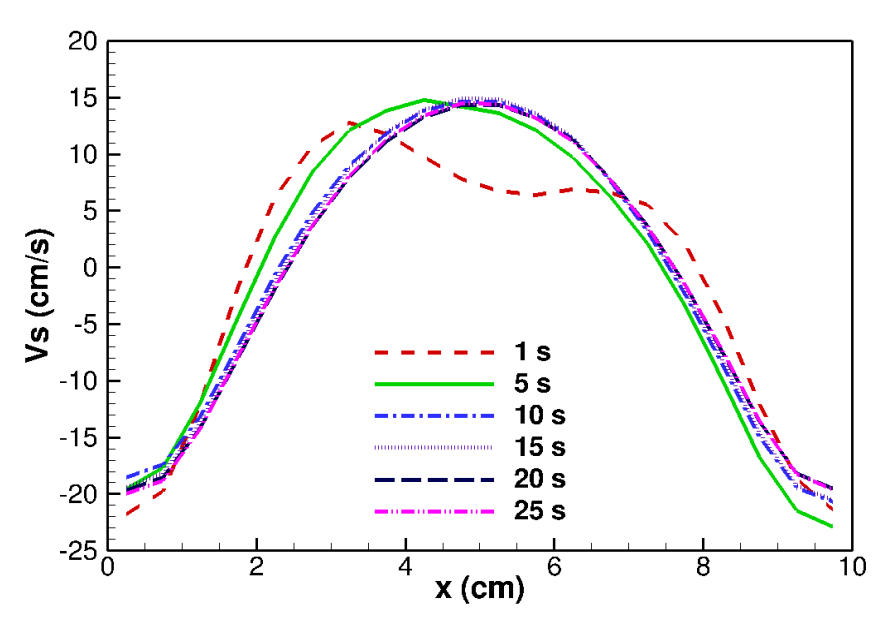


Figure 18. Variations of mean vertical particle velocity for different averaging time spans at the height of 50 mm ($t/d_p=20$).

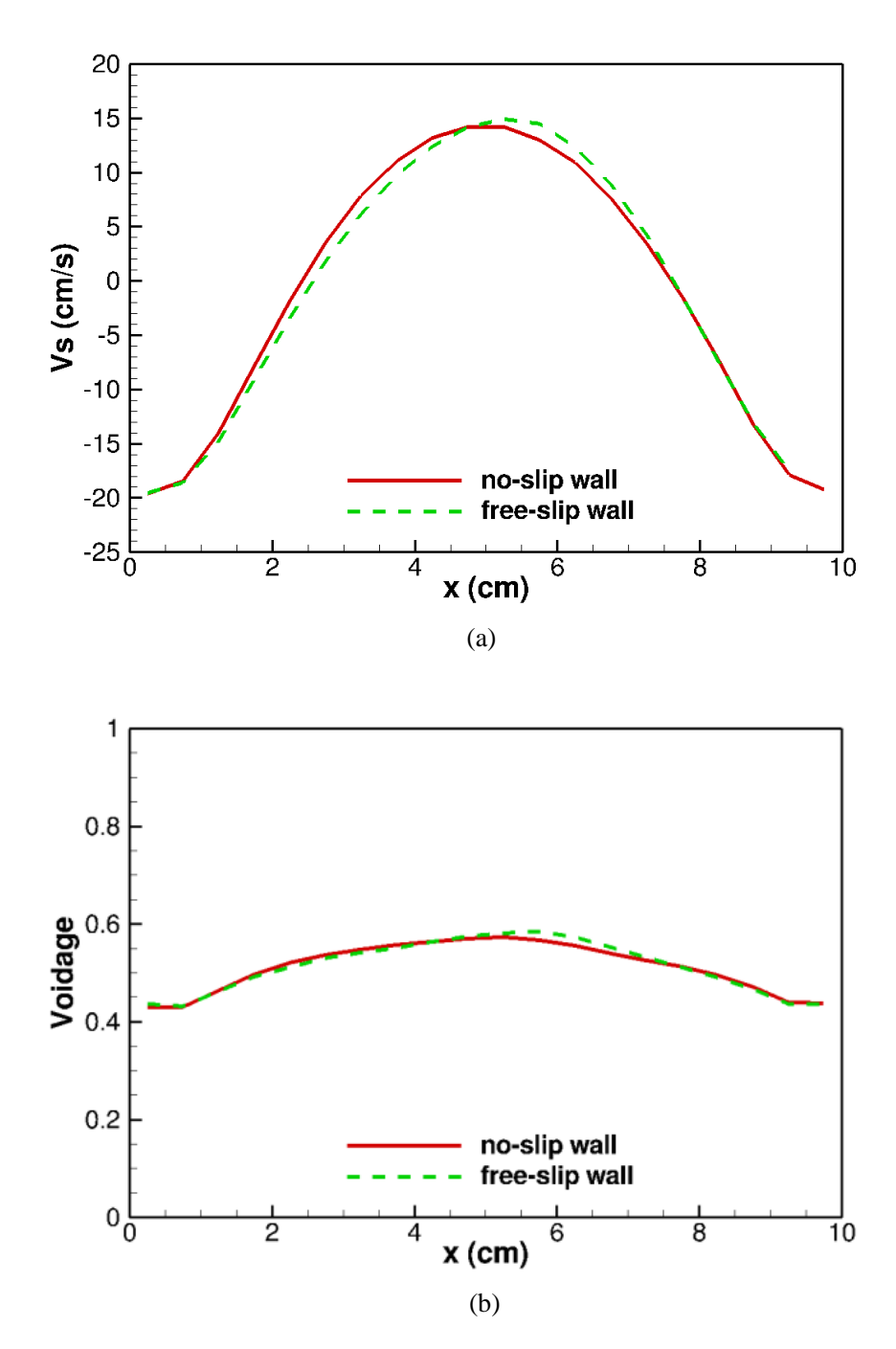
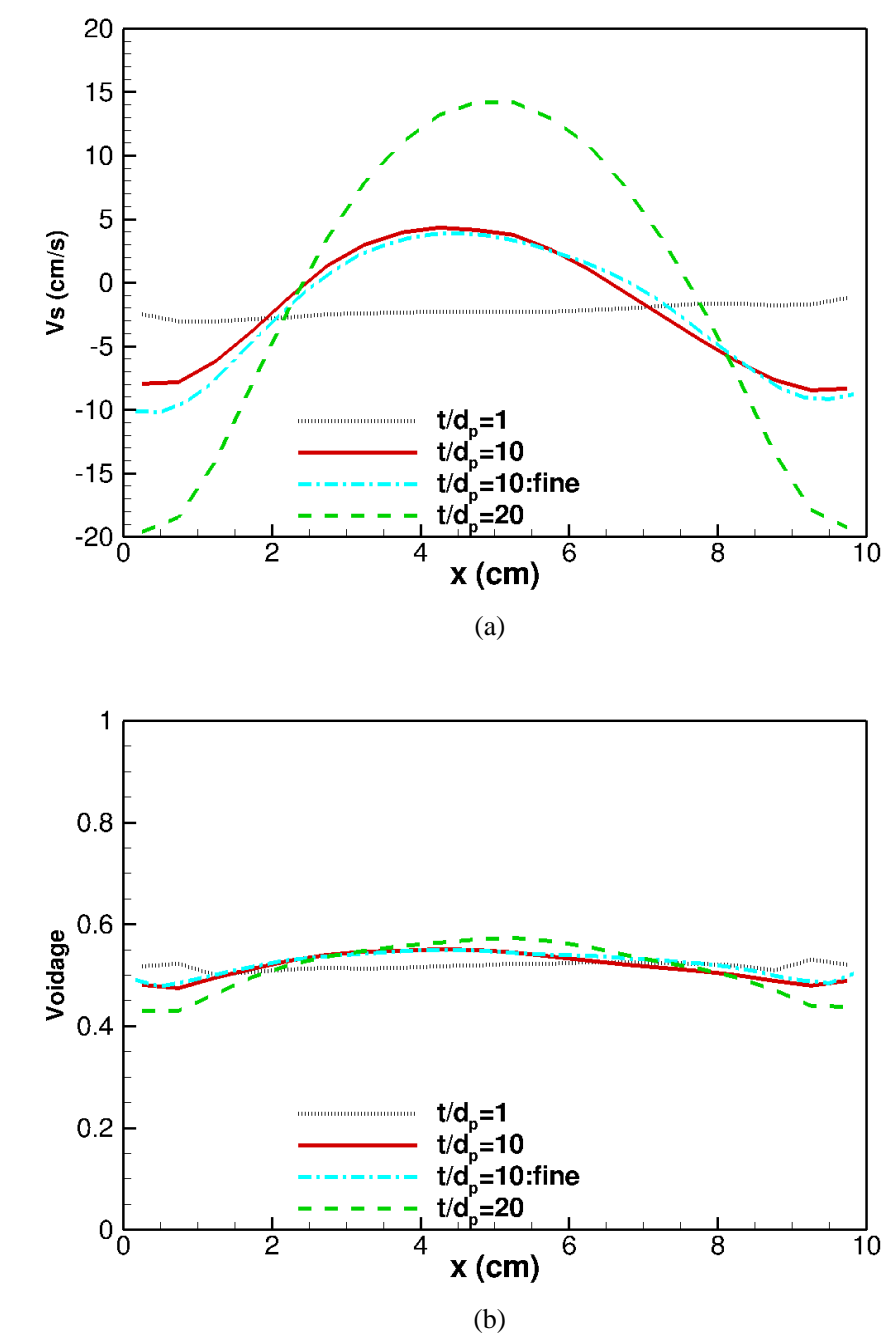


Figure 19. Lateral profiles of (a) vertical particle velocity and (b) voidage at the height of 50 mm for different wall boundary conditions for the gas phase.



(b) Figure 20. Horizontal profiles of (a) vertical particle velocity and (b) voidage, at height of 50 mm for different bed thicknesses.

Table 3. Parameters used in the MFIX-DEM simulations.

Property	Value	Property	Value
Particle diameter, d _p	1 mm	Particle density	2500 kg/m^3
Normal inter-particle	800 N/m	Normal particle-wall	800 N/m
spring constant		spring constant	
Tangential inter-particle	229 N/m	Tangential particle-wall	229 N/m
spring constant		spring constant	
Inter-particle restitution	0.97	Particle-wall restitution	0.97
coefficient		coefficient	
Inter-particle friction	0.1	Particle-wall friction	0.1
coefficient		coefficient	
Gas density	1.2 kg/m^3	Gas viscosity	1.8e-5 Pa.s

Table 4. Time-averaged particle heights and standard deviations for different bed thicknesses.

	$t/d_p=1$	$t/d_p=5$	$t/d_p = 10$	$t/d_p = 20$	$t/d_p = 40$	$t/d_p = 100$
<h>(cm)</h>	4.04026	4.472902213	4.16992	4.12329	4.2125	4.11026
δ (cm)	0.16756	6.83757E-08	0.20018	0.20997	0.3164	0.21778